Contents lists available at ScienceDirect

Talanta

journal homepage: www.elsevier.com/locate/talanta

The origin of the blue colour of Bronze Age vitreous materials: a spectroscopic approach

Jacopo Orsilli [a,b], Silvia Vettori [c,*], Francesca Giannetti [d], Emma Cantisani [c], Rachele Manganelli Del Fà [c], Cesare Carlo Allart [e], Francesco D'Acapito [b], Francesco Di Benedetto [c,e]

[a] Department of Materials Science, University of Milano Bicocca, Via Roberto Cozzi 55, 20125, Milan, Italy
[b] CNR-IOM-OGG c/o ESRF – The European Synchrotron, 71 Avenue des Martyrs CS 40220, Cédex 9, Grenoble, 38043, France
[c] Institute of Heritage Science, National Research Council of Italy (ISPC-CNR), via Madonna del Piano 10, Sesto Fiorentino, 50019, Florence, Italy
[d] Department of Earth Sciences, University of Florence, Via G. La Pira, 4, 50121, Florence, Italy
[e] Department of Physics and Earth Science, University of Ferrara, via Saragat 1, 44122, Ferrara, Italy

ARTICLE INFO

Keywords:
XAS
EPR
Glasses
Bronze Age
Chromophores
Valence states

ABSTRACT

An X-ray Absorption Spectroscopy (XAS) and Electron Paramagnetic Resonance (EPR) investigation of protohistoric blue vitreous materials was undertaken, aimed at ascertaining the valence state speciation of Cu and Co, suspected to play a role in the colour origin.

Five different glass artefacts coming from Paduli (Colli sul Velino, Rieti, Italy) were investigated. A bichrome blue and white vessel fragment represents the only *Natron glass*. The other four beads, instead, are *LMHK glass*. A relevant question deals with concentration, distribution, and valence states of the transition elements Cu and Co. Two out of the five colored objects, in fact, contain only Cu, whilst the others exhibit both Cu and Co.

A sample holder was specifically designed to ensure minimal invasiveness during XAS measurements. Multiple measurements (up to six) were performed for each sample at the Cu and/or Co edges to verify sample homogeneity. Fragments of the samples, when available, were investigated by EPR without manipulation to further characterize the Cu^{II} aliquot in the materials.

The XAS spectra provided significant information confirming the presence of the Co^{II} chromophore in the samples where this species is chemically more abundant, and identifying and quantifying the presence of the Cu^{II} chromophore. Cu^{II}, as revealed by EPR, appears in a distorted (4 + 2)-fold coordination and partly clustered to form pairs.

This spectroscopic approach, combining XAS and EPR techniques, proves to be successful in the characterization of Co- and Cu-based blue colors in the glasses of the Bronze Age, highlighting the high skill reached in the production.

1. Introduction

Over recent decades, the analytical study of ancient glass has allowed an extraordinary advance in understanding the ancient world [1]. Chemical, mineralogical, and textural analyses, together with geochemical isotopic signatures, allow identification of the different recipes, the level of available technology, the nature and origin of the raw materials, and can also help to follow the diffusion of the manufactured objects or to locate geographically the primary glass workshop [2].

Glass is a synthetic material obtained by fusing high-silica rocks (quartz or sand) with fluxing agents to lower the melting temperature (usually soda or potash obtained from natural deposits or plant ash). The chemical compositions of ancient glasses, considering both the raw materials and the coloring recipes, vary with the place and period of production [3,4].

Apparently, glass-making and glass-working largely date back to the 11th and 10th centuries BC, showing in particular the production of

This article is part of a special issue entitled: Cultural Heritage Analysis published in Talanta.

* Corresponding author.
E-mail address: silvia.vettori@cnr.it (S. Vettori).

https://doi.org/10.1016/j.talanta.2026.129622
Received 1 September 2025; Received in revised form 19 January 2026; Accepted 2 March 2026
Available online 3 March 2026

opaque red, opaque dark blue, and transparent light blue glass [5].

The main factors influencing the colour exhibited by a glass are the presence of a particular metal ion, usually a transition metal, its oxidation state, and electronic configuration [6–9]. These metals, indeed, absorb characteristic frequencies in the visible region as a result of the d–d electronic transitions. As a result, the most common colorants in glasses were iron, manganese, copper, and cobalt [10].

As not only the elemental species, but also the oxidation state, coordination, and local order are parameters that can influence the hue and intensity of the colour shown by a glass, X-ray Absorption Spectroscopy (XAS) can be considered a suitable technique to investigate the properties of the chromophore elements. Besides, XAS is an element-specific non-invasive technique, can be applied in air with micro or macro beams on different kinds of samples (crystalline and amorphous solids, liquids, and gases), without any need for treatment, making it extremely suitable for studying archaeological and historical artefacts [11–13]. Here, the application of XAS to the study of historical glass has been devoted to unravelling the origin of the glass colour [14–19].

EPR is applied in the Cultural Heritage field with different purposes, as e.g. for dating (quartz, carbonates), for chemical characterization (pigment, glass, organic binders), and for provenancing marbles [20, 21]. EPR spectroscopy has specifically applied also to archaeological materials ([22] and reference therein). EPR has proved to be a promising tool towards a better comprehension of the complex mechanisms involved in the colouration of glasses, because of its capacity to give information on the oxidation states of the chromophorous metallic ions [23]. The features of the EPR spectra, in fact, could be successfully associated with the presence and abundance of the paramagnetic coloring ions (namely iron, manganese, and copper) and to their oxidation states.

In this study, an X-ray Absorption Spectroscopy (XAS) and Electron Paramagnetic Resonance (EPR) investigation of five protohistoric vitreous materials coming from Paduli (Colli sul Velino, Rieti, Italy) [24–28], was undertaken, aimed at ascertaining the valence state speciation of the transition elements (Cu and Co) suspected to play a role in the origin of their blue colour.

2. Materials and methods

During the survey and digs, about 20 vitreous materials were found in the protohistoric and peri-lacustrine archaeological site of Paduli (Colli sul Velino, Rieti, Italy), but thanks to non-destructive and non-invasive techniques (*p*-XRF, FORS, and XRD), adopted to provide a first detailed characterization, a specific selection of the more significant and representative objects has been possible, for further micro-destructive investigations [28]. The case study is thus provided by 5 different glass artefacts (shown in Fig. 1), dating from the Middle Bronze Age to the Early Iron Age: two beads from blue to turquoise (AB_2 and AB_9); a "star" bead with light and dark blue bands (STAR); a vessel fragment, bichrome blue and white (Vf) and a blue barrel bead with white spiral decoration (BB). The description of the samples is summarized in Table 1. The 5 glass artefacts here considered were analyzed for their microstructure information, chemical composition, and chromophores identification through a combined SEM-EDS and EMPA study by Vettori et al. [28]. Further LA-ICP-MS and Sr-Nd-Pb isotopic ratios investigations are in progress (Giannetti et al., *in preparation*). The combination of non-invasive and micro-destructive techniques allowed us to identify three main glass types: (I) the bichrome vessel fragment Vf displays a composition typical of *Natron glasses*; (II) the samples AB_2, STAR, and BB have a Low Magnesium High Potassium composition (*LMHK glasses*); (III) AB_9 presents a HIGH-K composition [28]. If instead we consider the type and concentration of chromophores (obtained through *p*-XRF, FORS and EMPA analyses) we can divide the samples into two distinct groups: I) AB_9 and STAR display a light blue/turquoise color and show an extremely high Cu concentration and negligible amounts of Co; II) AB_2, BB, and Vf display a darker blue color, associated with significant amounts of both Co and Cu.

2.1. X-ray Absorption Spectroscopy (XAS)

Archaeological glass artefacts were investigated by means of XAS in fluorescence mode. The measurements were carried out at the Co and Cu K-edges (7709 and 8979 eV, respectively) at the Italian CRG Beamline Lisa (BM08) at the European Synchrotron Radiation Facility (ESRF, Grenoble, France) in the ESRF experiment HG217 [29]. Fluorescence yield was collected through a 12-element N_2-cooled HPGe detector.

Table 1
Description and grouping of the samples analyzed with the relative Cu and Co concentration, measured with EMPA spot analysis.

Sample	Period	Morphology	Glass type	Colour	Cu [mg/kg][a]	Co [mg/kg][a]
AB_9	RBA 1 –EIA 1B	Anular bead	high-K	Turquoise	25484	Bdl
AB_2	RBA 1 – EIA 1B	Anular bead	LMHK	Dark blue	2556	1573
STAR	EIA 1A	Star bead	LMHK	Light blue	20611	Bdl
				Dark blue	25324	472
Vf	EIA 1A?	Vessel fragment	Natron	Dark blue	1198	1258
				Opaque	80	157
BB	EIA 1A	Barrel bead	LMHK	Dark blue	7749	786
				White	1358	Bdl

[a] Recalculated from EMPA wt% oxide analyses of [28]. EMPA analyses have an average uncertainty of 5% for both Co and Cu. Bdl: below detection limit, RBA: Recent Bronze Age, EIA: Early Iron Age.

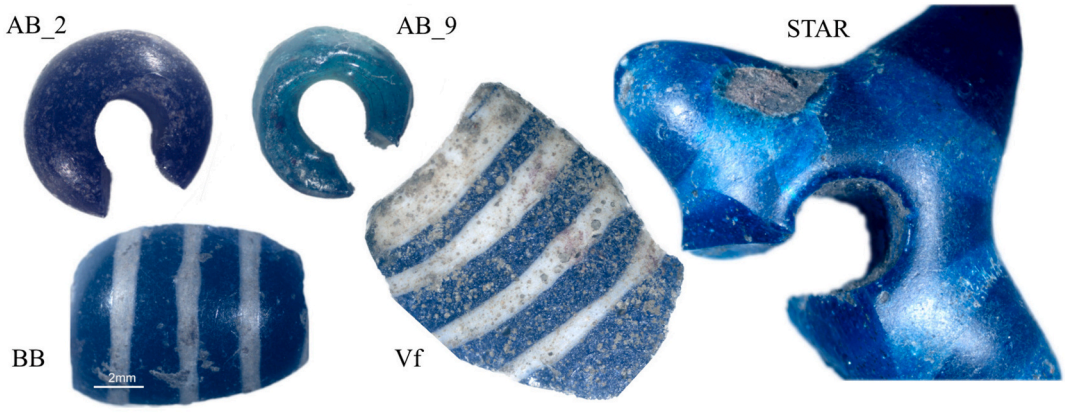

Fig. 1. Five glass artefacts studied.

Reference materials (Co and Cu metal foils) were placed in a second experimental chamber, located downstream from the first one, to provide accurate energy calibration. The beam flux before the sample, after it, and after the reference foil was measured using 1 bar N_2-filled ionization chambers with an applied voltage of 1 kV. The energy of the X-ray beam was selected by a fixed exit monochromator with a pair of Si (111) crystals (energy resolution $\Delta E/E \approx 1.1 \times 10^{-4}$). At the same time, Si mirrors were used for harmonics rejection ($E_{cutoff} \approx 15$ KeV). Spectral acquisitions were set up to have significant energy resolution both in the X-ray Absorption Near Edge Structure (XANES) and Extended X-ray Absorption Fine Structure (EXAFS). Accordingly, the step size in the XANES region was 0.5 eV; the post-edge EXAFS region of the spectrum was acquired with a fixed k-step width of 0.05 Å-1. The experimental chamber, which housed the sample holder containing the archaeological specimens, was filled with He to minimize unwanted attenuation by the atmosphere. Measurements were carried out at room temperature. For EXAFS and XANES interpretation, a set of relevant mineral and glass standards was also investigated. A first subset of pure chemicals was considered, which included oxides and sulfides of the two absorber elements: CoO, $LiCoO_2$, Co_3O_4, $CoFe_2O_4$ for Co; CuO, Cu_2O, Cu_2S. The spectra of standards belonging to this group were recorded under the same environmental conditions, but in transmission mode. Materials were pelletized after having mixed an appropriate amount of sample with 100 mg of cellulose powder, the absorption of which under the experimental conditions is negligible. After being measured in fluorescence with XAS to confirm the presence of only one Cu species (Cu^I or Cu^{II}), two synthetic glass samples GS1 and GS2, were employed as reference.

The analysis of the XAS spectra was performed using Athena and Artemis software, part of the Demeter package [30] and Larch [31]. Namely, the raw absorption spectrum was energy calibrated, background subtracted, and normalized, and the XANES and EXAFS spectra were extracted. XANES spectra were investigated through a Linear Combination Fit (LCF) procedure operated both on the normalized absorption and the first derivative, using as end-members the mineral and glass references. The LCF procedure was accomplished through the routine built-in the Larix tool, operated in the energy range −20 to +45 eV (evaluated regarding the edge position) of the experimental μ(E) spectra of the unknown phase compositions. The reference spectra were used as primary components, and their weights were forced to vary between 0 and 1 while their edge positions, as well as the total weights sum, were left free to vary.

Theoretical EXAFS paths of cobalt and copper were calculated using feff6 [32] starting from the models of Co_3O_4 reported by Kotousova, [33], CuO (tenorite) reported by Wyckoff [34], Cu_2O (cuprite) reported by Neuburger [35], and Cu_2S (chalcocite) reported by Evans [36], using Muffin Tin potentials and the Hedin–Lundqvist approximation. Both the edges were analyzed in the k range, using a k^2-weight and considering a range of 3 – 10 $Å^{-1}$ to calculate the FT. The latter was fit in the R space considering a range of 1 – 3 Å. To refine the coordination number, the interatomic distance, the number of neighbors and the valence have been constrained using the Bond Valence Method (BVM) [37,38].

2.1.1. Sample holder design

To properly investigate the set of available archaeological samples using the XAS technique, a suitable sample holder has been conceived, designed, and realized. In particular, the holder fulfils three requirements.

1) allocating the specimen in a free volume large and deep enough to host it, while maintaining the specimen surface in the focal plane of the investigation;
2) minimizing the interactions between the specimen and the holder, to preserve the integrity and pristine conditions of the specimen;
3) being fully compatible with the beamline setup and motors, to allow both fluorescence and transmission measurements.

According to these specifications, the sample holder was designed as a parallelepiped with three large open cavities (20 × 20 × 10 mm^3 in size) (Fig. S1), able to host at least three different specimens simultaneously. The parallelepiped stands over a base, which acts as a connection, through a dovetail (Fig. S1c), to the motors present in the experimental chamber of the beamline. According to the motor setup of the experimental chamber, the holder is allowed to move vertically (thus selecting which one of the three cavities is put in front of the X-ray beam) and turn around the vertical axis (thus selecting the orientation needed for Transmission and Fluorescence measurements). As the axis rotation axis lies in the front surface of the cavities of the holder, any chosen sample region on that surface maintains into the beam focus (Fig. 2). The three-dimensional modeling of the sample holder was designed out of a dimensioned drawing. The two-dimensional project was planned with particular attention to the requirements described above. It was decided to work in a CAD environment for the three-dimensional rendition of the older. Creating a 3D solid from an object that encloses an area is a straightforward operation.

Objects can be extruded orthogonally from the plane of the original object, in a specified direction or along a selected trajectory. Once the individual objects were drawn and extruded, the solid editing commands made available by the program were used. By subtracting a group of existing solids from another overlapping group, it is possible to create a new 3D solid. The model was then exported in ‘stl’ format. The.stl model was imported into the Ultimaker Cura program which divides the designed model file into layers, generating a specific code for the 3D printer. Finally, the sample holder was 3D printed using a Voxelab Aquila X2.

The archaeological samples were investigated without any manipulation, using a Kapton tape to place them on the holder's virtual focus surface. Kapton was chosen because it is nearly transparent to X-rays, thus limiting the interference with the fluorescence investigations. To avoid any accidental loss during the measurement, a second tape was put on the opposite end of the holder cavity (Fig. 2c).

2.2. Electron Paramagnetic Resonance spectroscopy (EPR)

Aliquots of microfragments (obtained for detailed and micro-destructive previous analyses, see Ref. [28]) of 3 glass artefacts (i.e. Vf, BB, and STAR) were analyzed by EPR without further manipulation. The aliquots were inserted in amorphous silica tubes and then transferred into the resonant cavity of the spectrometer. The chosen tubes allow avoiding the presence, in the glassy matrix, of transition metal impurities, which would likely interfere with the EPR spectra of the samples. The EPR spectral measurements were carried out using a conventional Bruker ER 200D-SRC, operating at ~9.5 GHz (X-band). All spectra were registered at room temperature according to the following conditions: 0.8 mT modulation amplitude, 100 kHz modulation frequency. The post-amplification gain setup was optimized, sample by sample, maximizing the signal-to-noise ratio. Frequency was calibrated through the reference signal of the DPPH (1,1-diphenyl-2-pycrylhydrazyl) radical, used as an external standard. Panoramic spectra were registered in the 0–1000 mT magnetic field range, with a field step of 0.244 mT and at a scan speed of 5 mT/s. Detailed spectra were then registered limiting the magnetic field range close to the paramagnetic signals observed in the panoramic spectra: typically, detailed spectra were registered in the 230–430 mT magnetic field range, with a field step of 0.097 mT and at a scan speed of 1 mT/s.

3. Results

3.1. XAS of the Co K-edge

The XAS spectra of the Co-containing samples (AB_2, BB, and Vf) are shown in Fig. 3. For all the samples, we observe that the energy and shape of the pre-edge peak, the edge position, and the XANES features

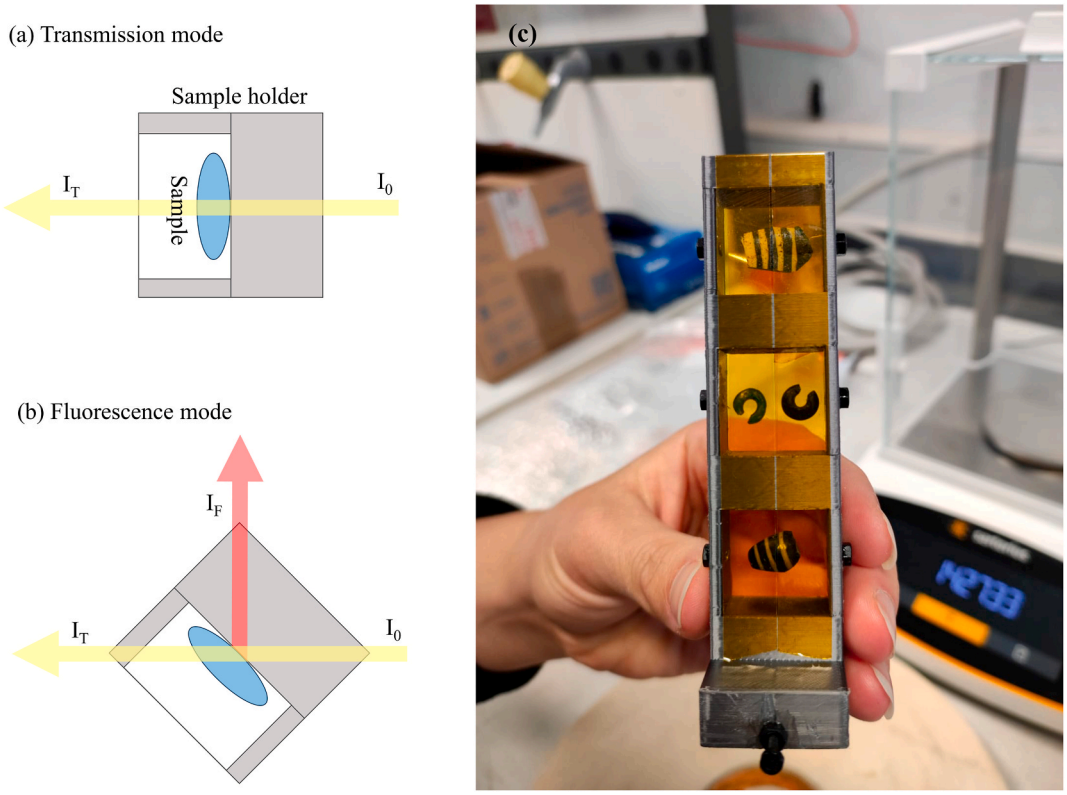

Fig. 2. Geometric setup of the sample holder, containing a specimen, with respect to the incoming X-ray beam and to the active detectors in both the transmission (a) and Fluorescence (b) modes. (c) photograph showing the sample holder with 4 mounted specimens, stick by the Kapton tape.

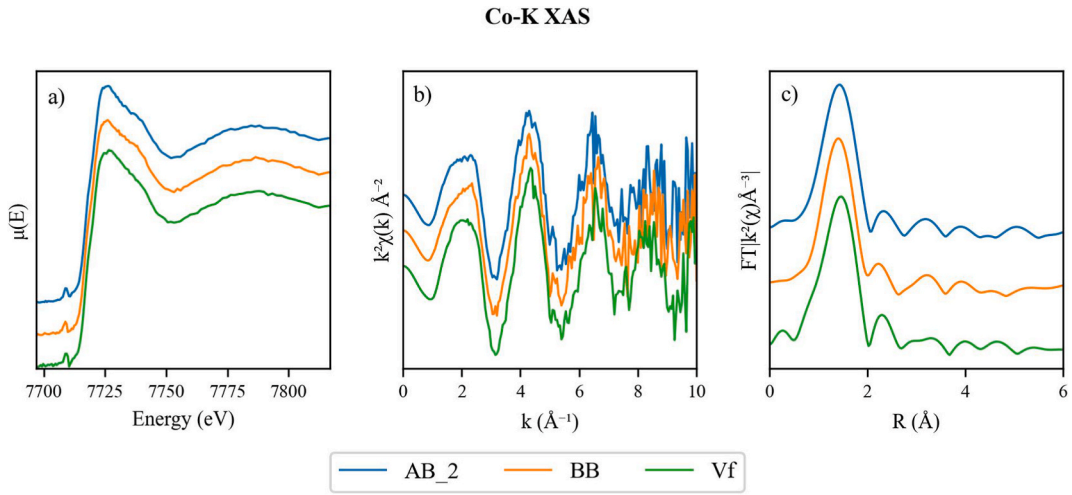

Fig. 3. (a) Co K edge XANES, (b) EXAFS, and (c) EXAFS Fourier transform spectra of the three investigated Co-bearing samples.

are very similar (Fig. 3a). This suggests that cobalt is occurring in the same chemical environment. In particular, the pre-edge features can convey significant information to identify the element valence state and coordination number. The peak position energy, 7709.2(5), and its normalized intensity value, 0.067(8), are in full agreement with what is expected for Co^{II} in a tetrahedral coordination [39]. This feature has been commonly observed in glasses of historical or archaeological relevance [40]. Interestingly, this evidence is observed as a constant feature of multiple analytical points registered in each sample. Therefore, one can consider the occurrence of 4-coordinated Co^{II} as a general feature of the samples investigated.

This result can be confirmed from the EXAFS spectra and their Fourier Transform, Fig. 3b and c. EXAFS spectra were fit using a structural reference of Co_3O_4, to consider both the tetrahedral and octahedral coordinations. The value of S_0^2 was fixed at 0.74, and the BVM was employed to constrain the coordination number with the interatomic

Table 2
Results of the EXAFS fit of the Co K-edge, in brackets the error on the last digit.

Sample	Bond	N	R [Å]	σ^2[× 10^3] [Å^2]	e_0 [eV]	r
AB_2	Co–O	4.0(2)	1.95(2)	2(1)	2(2)	0.024
BB	Co–O	3.9(1)	1.94(1)	2(1)	0(1)	0.014
Vf	Co–O	4.1(2)	1.96(2)	2(3)	0(2)	0.027

distance and the valence. The valence was fixed at 2 and the starting parameter, $R'_{Co^{II}-O}$, was fixed at 1.692 Å. The results, summarized in Table 2 and shown in Fig. S2, show that in the samples, Co is present with a coordination of 4 (nominal distance 1.95 Å) [41], as no fit of the 6-coordinated path (2.15 Å) was possible.

3.2. XAS at the Cu K-edge

The first experimental finding obtained from the single analytical points of the XANES investigation carried out on the 5 archaeological samples is the variability of the spectral features of the Cu K-edge. With the notable exception of the Vf sample, spectra from all other samples revealed differences that prevented them from being considered fully homogeneous. Fig. 4 shows the main spectral types observed in the dataset, exemplified by some measured points. These same differences, however, are not observed in the EXAFS regions, except for sample AB_2. For this reason, before the EXAFS analysis, the spectra were merged to increase the S/N ratio of the EXAFS oscillations.

In the XANES region, one can observe that two similar spectra (i.e., those of AB_2_b and c and AB_9 in Fig. 4) are discriminated by the relevance of a pre-edge feature at ~8984 eV, coupled to a less evident spectral change between 8995 and 9005 eV. These changes were already observed in Cu-bearing glasses by Refs. [17,42], who attributed, in particular, the pre-edge peak at 8984 eV to a 2-coordinated Cu^{I} species diluted in the glassy matrix. The third spectral type, represented in Fig. 4 by the AB_2_a spectrum, is different from the others and marks the presence of different Cu-bearing phases in the sample. We decided to gain further insight (Fig. 5) into the two general rules of differentiation in our dataset, namely the change in the redox state of Cu in the glass and the presence of additional phases in the sample, using the references GS1, GS2, to evaluate the amount of Cu^{I} and Cu^{II} in the glassy matrix, and Cu_2S, which was already detected by SEM-EDS investigation [28]. To confirm that the three chosen standards could be employed to fit the samples' spectra, we previously performed a PCA analysis on the samples to create a new spectral base, and the three main components were then employed to fit the reference spectra, as shown in Fig. S3.

Having defined the three reference compounds, we performed a LCF procedure, optimized using the least squares method, as shown in Fig. S4. From the data listed in Table 3, one can conclude that chalcocite is mainly present only in the AB_2 sample, with a variable contribution in the matrix, and with a lower concentration in samples AB_9 and Vf. Conversely, in all investigated samples, Cu is mainly, or exclusively, present in the glass fraction, but with significant changes in the valence states. Fig. 6 graphically depicts this variability. Concerning Cu speciation in glass, the samples AB_2, AB_9, and Vf show a major presence of Cu^{I}, while the STAR shows a major concentration of Cu^{II}.

The EXAFS spectra were fit with Artemis, the fixed parameters

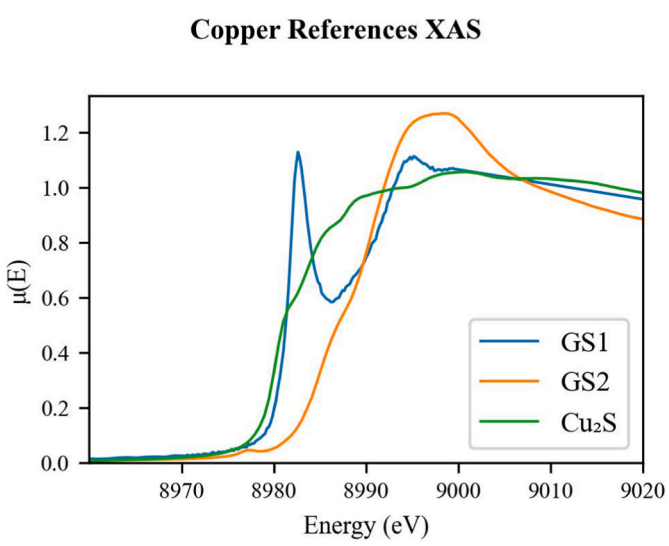

Fig. 5. Cu K edge XANES spectra of the three relevant reference compounds used for the LCF procedure.

Table 3
Results of the LCF of the XANES spectra collected at the Cu K-edge.

Data	GS1	GS2	Cu_2S	Total	Res. [× 10^{-4}]
AB_2a	14.7	2.9	86.0	103.7	3.40
AB_2b	39.7	29.9	24.8	94.4	0.48
AB_2c	62.0	19.6	15.7	97.3	0.77
AB_9a	59.4	31.5	6.5	97.3	1.41
AB_9b	61.8	28.8	7.4	97.9	1.99
AB_9c	55.5	35.2	0.0	90.7	2.47
BB	57.9	36.7	2.0	96.7	0.87
STAR_a	36.7	64.8	0.0	101.5	1.71
STAR_b	34.1	66.6	0.0	100.7	0.94
STAR_c	37.4	58.5	4.2	100.1	0.64
STAR_d	32.6	64.4	3.2	100.3	0.43
STAR_e	33.8	63.9	2.4	100.1	0.40
STAR_f	34.9	65.5	0.0	100.3	0.62
Vf	69.1	19.4	10.0	98.6	1.51

employed in the fitting, and the results are summarized inTable S1 and Table 4, respectively.

For the first shell, we considered a 2-coordinated Cu^{I}–O, a 4-coordinated Cu^{II}–O, and a 3-coordinated Cu^{I}–S structure depending on the sample. Due to the high amount of Cu^{I} in the samples, for samples AB_2, AB_9, BB, and Vf, we fit only the Cu^{I}–O. The detection limit of a secondary valence state in the EXAFS analysis is, in fact, reported to be of

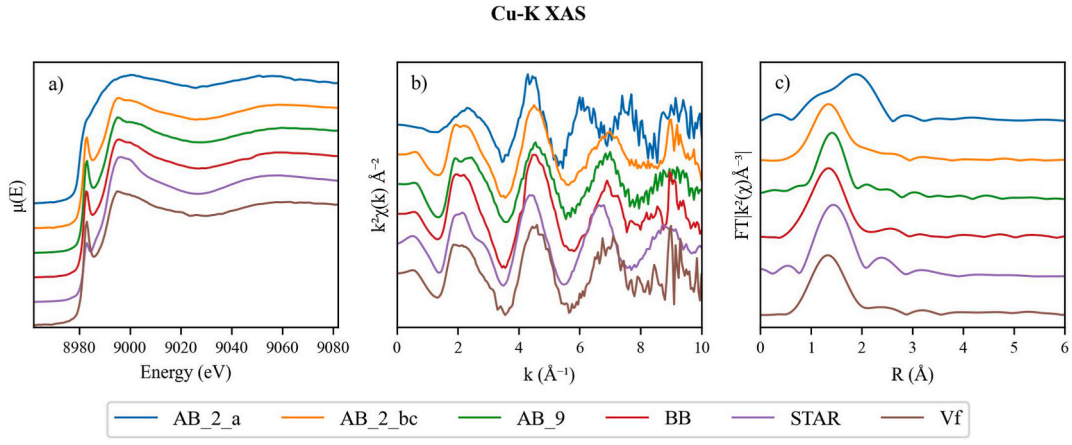

Fig. 4. Examples of Cu K-edge XANES spectra of the investigated glasses, exhibiting the large spectral variability of the whole dataset.

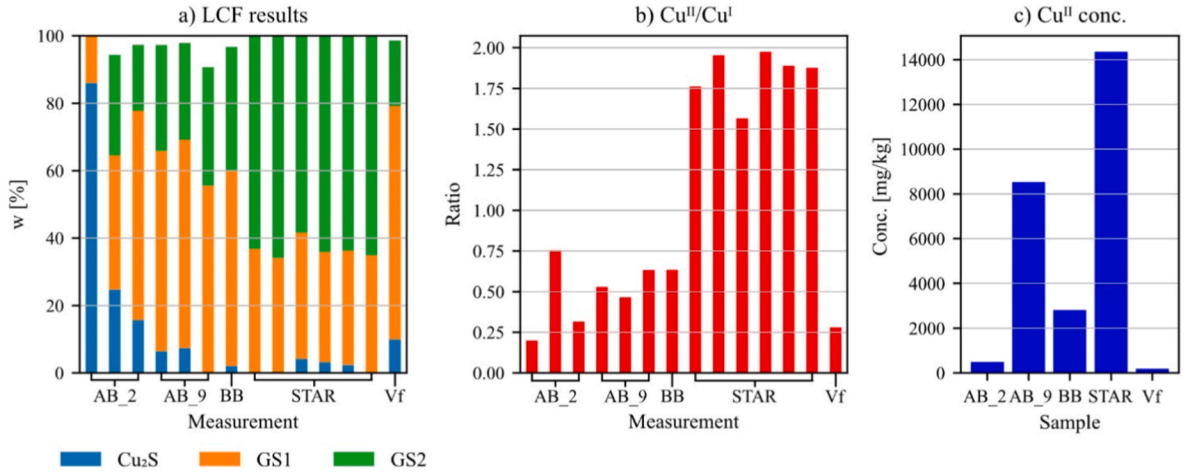

Fig. 6. a) bar diagram exhibiting the variability in the Cu speciation through the results of the LCF procedure; b) the ratio of the copper phases in the glassy matrix (excluding Cu_2S); c) the estimated Cu(II) concentration in the glass samples is calculated from the combination of the information contained in Tables 1 and 3

Table 4
Results of the EXAFS fit of the Cu K-edge, in brackets the error on the last digit.

Sample	Bond	N	R [Å]	σ^2[× 10^3] [Å^2]	e_0 [eV]	r
AB_2a	Cu^I–O	2(1)	1.9(2)	1(2)	11(9)	0.236
	Cu^I–S	3(1)	2.4(1)	1(1)		
AB_2bc	Cu^I–O	2.0(1)	1.85(3)	4(2)	6(4)	0.047
AB_9	Cu^I–O	2.0(1)	1.85(2)	4(1)	8(3)	0.044
BB	Cu^I–O	2.1(1)	1.86(2)	2(1)	9(3)	0.030
STAR	Cu^I–O	1.7(3)	1.80(7)	4(2)	7(2)	0.017
	Cu^{II}–O	3.8(1)	1.92(1)	4(2)		
Vf	Cu^I–O	2.0(1)	1.86(3)	3(2)	8(4)	0.052

the order of some wt% [43]. For the STAR sample, both monovalent and divalent species were considered, while for the spectrum AB_2a, we considered the monovalent Cu–S and Cu–O bonds. In both cases, the concentration of the phases was fixed using the LCF results.

The results, depicted also in Fig. S5, show that the coordination number and the Cu–O and Cu–S interatomic distances are compatible with those of the references employed, even considering only one valence state. However, the fit of the measure AB_2a shows a great uncertainty in the coordination number, distances, and Debye-Waller factor (which are correlated), due to the noise of the data and the limited amount of EXAFS oscillation employed. Monovalent copper is thus 2-coordinated, while divalent copper appears to be at least 4-coordinated.

3.3. EPR

The EPR spectra of the investigated fragments, although different, reveal some common patterns (Figg 7 and S6).

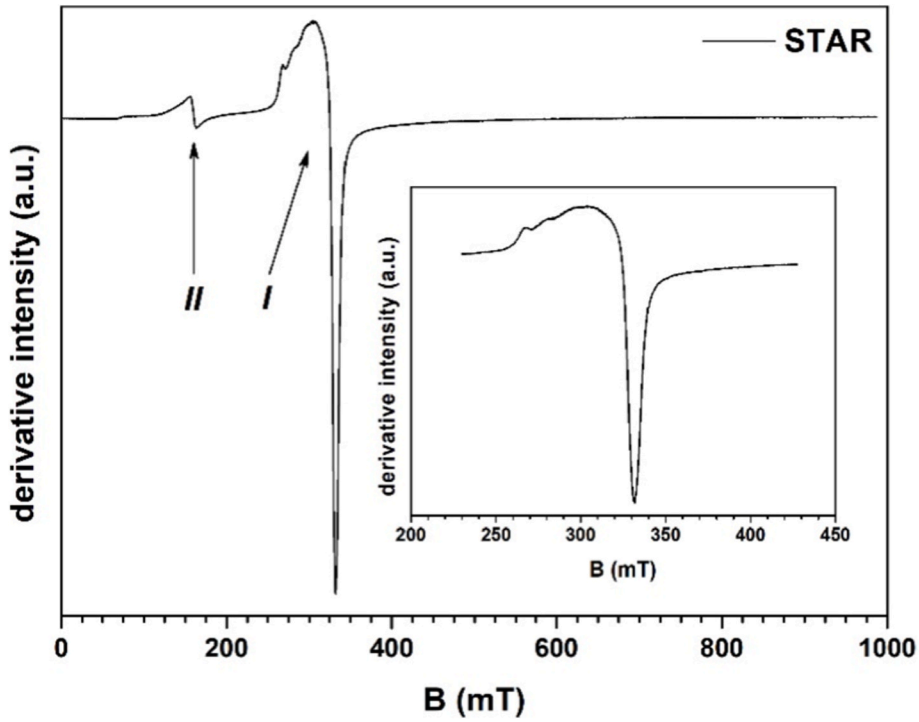

Fig. 7. Panoramic X-band EPR spectra of the STAR sample. Spectra were registered at room temperature. In the inset, high resolution EPR spectrum of the main signal. The I and II labels mark the different signals discussed in the text.

The most intense signal is an asymmetric line centered at ~315-320 mT (I), always accompanied by a second line (less intense but, in this case, definitely more symmetric) occurring at ~160 mT (II). A similar pattern is revealed by the spectrum of the BB sample, where signals close to the I and II species in STAR are apparent. In the BB spectrum, both species are broader and less intense. In Vf spectrum, signals in the I and II regions are still present, the first one exhibiting a different asymmetric shape, and an additional signal, occurring at ~255 mT (labelled as III) is present. Concerning the intensity, as far as one can observe from the signal-to-noise ratio, Vf and BB spectra are of almost poor quality (the peak-to-noise ratio decreases from ~575 in STAR to ~10 BB and Vf): this could be attributed to an unfavourable combination of few amount of sample, and of the dilution of the paramagnetic centres (somehow in line with the total Cu^{II} concentration Fig. 6). We started our analysis from the I signal of the STAR spectrum, due to its definitely greater peak-to-noise ratio. The main signal at ~320 mT, corresponding to an average g_{eff} value of ~2.12, is in line with the values typically reported for isolated Cu^{II} (e.g. Ref. [44]). This is, of course, in excellent agreement with the Cu presence revealed by the chemistry of the glass [28], and also by the XAS investigation. The quality of the spectrum of the STAR sample allowed us to get a deeper insight into the nature of the spectrum due to Cu^{II} ions. The spectrum was reproduced by numerical simulations, the results of which are shown in Fig. S7. The best fit simulation was achieved accounting for two different species, one being approximately 1/3 less relevant than the other. The less abundant species exhibits an axial anisotropy ($g_{\|} = 2.377$; $g_{\perp} = 2.085$; $a_{\|} = 142{\cdot}10^{-4}$ cm^{-1}; $a_{\perp} = 5{\cdot}10^{-4}$ cm^{-1}), whereas the most abundant species exhibits a pseudoaxial rhombic anisotropy ($g_1 = 2.350$; $g_2 = 2.120$; $g_3 = 2.085$; $a_1 = 102{\cdot}10^{-4}$ cm^{-1}; $a_2 = a_3 = 5{\cdot}10^{-4}$ cm^{-1}). The occurrence of different species, all of them tracing isolated Cu^{II} ions in the glass, confirms the complex crystal chemistry of this ion in the variable chemical and structural environment provided by the glassy matrix. Interestingly, the best fit Hamiltonian parameters of both species, in particular the parallel hyperfine interaction constant and the parallel g factor, following Peisach and Blumberg's classification method [44,45], point to Cu^{II} ions occurring in a distorted hexacoordinated local environment. Indeed, the differences between the two contributions needed to reproduce the I signal of the STAR spectrum can be attributed to two hexacoordinated Cu^{II} species, exhibiting different local distortions. In analogy, the I signals in the spectra of BB and Vf samples could be attributed to isolated Cu^{II} ions in the glassy matrix, exhibiting different degrees of distortion. In particular, one can observe that the rhombicity of the I signal in the Vf spectrum is definitely higher.

Concerning the II signal, its localisation (B~160 mT and g_{eff}~4.2) is in the range of values typically reported for rhombic Fe^{III} [46]. The total Fe content of the STAR, BB and Vf samples range between 0.45 and 1.02 FeO wt% [28]. However, its symmetry and the almost perfect 1:2 relationship between the g_{eff} values in the I and II species suggest another possible explanation. The II species could be, in fact, the forbidden half-field transition of the I species, corresponding to Ref. [47]. The occurrence of this second signal, indeed, could be related to the occurrence of Cu pairs in the glass matrix. Because similar occurrences are also observed in the other two samples, we suggest that the co-presence of Cu^{II} isolated ions and pairs is common in all the investigated materials.

Concerning the III signal, present only in the Vf spectrum, its attribution is uncertain. The most likely explanation, accounting for its g_{eff} value, could be due to some superparamagnetic cluster in the sample [48]. Another possible explanation could be assuming that the I and III signals in this spectrum are due to a single species, whose spectral structure is here revealed. Owing to the presence of several paramagnetic ions in the chemical formulation of the glass, which could cluster together, the exact nature of this contribution remains uncertain.

4. Discussion

On the basis of the spectroscopic results, the two main species revealed as potential chromophores for the considered glasses are Co^{II} and Cu^{II}.

The characteristics of Co^{II} are well depicted by XAS spectroscopy: the XANES and EXAFS features reveal that Co in these samples is divalent and occurs in a tetrahedral coordination. This ion is well described as a chromophore, inducing a blue-violet coordination [40,49]. This ion is reported to be effective in inducing the glass colour through a strong absorption in the red-orange region of the visible spectrum. However, the molar extinction coefficient was found to vary according to the type of glass network beyond the first coordination shell [40]. Here, the chemical composition of the glasses suggests that four out of the five samples are actually rich in K, whereas the fifth one (Vf) is rich in Na [28]. Indeed, even if attempting to relate to a conventional molar extinction coefficient is unhelpful, according to Ref. [40], one can state that the tetrahedral Co^{II} in AB_9 and BB can surely act as an efficient chromophore, whereas in Vf it could be considered slightly less efficient.

Conversely, the features of the Cu^{II} chromophore (including in this definition only the aliquot of isolated Cu^{II} ions in the glass) are devised from the combination of the XAS and EPR spectroscopic information. In this case, the chromophore is revealed as widely diffused in all the investigated samples, although associated with additional species (namely, Cu^{I}, which, however, does not contribute to the formation of the blue colour). From the comparison of the EXAFS results with the interpretation of the Zeeman and hyperfine anisotropies from the EPR investigation (carried out on the STAR sample), a distorted octahedral coordination (likely a 4 + 2 coordination shell) appears favoured. This result is again in line with previous findings on Cu^{II} chromophores on ancient glasses [14,40,50].

On the basis of the presence and abundance of the two identified blue chromophores, the five analyzed samples can be divided into three groups (among them, the first one is divided into two subgroups).

1a) The samples AB_2 and Vf contain ~1000 mg/kg Co or more. In all these samples, XAS investigations reveal that Co is occurring in the same valence state and coordination environment (within error). The contribution of this chromophore to the overall appearance of the samples results thus highly relevant. These results are thus in line with the results already published by our group [28]. In all these samples, the Cu content is below 2500 mg/kg, and that of Cu^{II} is above 1200 mg/kg;

1b) The sample BB is peculiar because, on one hand, the XAS results concerning the Co valence state and environment closely reproduce what has already been described for the subgroup #1a samples. On the other hand, however, in this sample, the Cu content is above 7500 mg/kg, of which ~3000 are Cu^{II}. It appears, thus, that the possible effect due to an additional chromophore, Cu^{II}, cannot be safely ruled out. For this reason, this sample cannot be grouped with the #1a subgroup samples.

2) In AB_9, the total amount of Co is too low (below the detection limit) to consider this species as a potential chromophore. Conversely, the total Cu content is definitely higher (~25000 mg/kg). According to the XANES information, ~1/3 of it is occurring as Cu^{II} (~9000 mg/kg). Even if undoubtedly in this sample the blue hue is given by the presence of a relevant amount of Cu^{II}, it is notable that the Cu^{II}/Cu^{I} ratio is almost in line with the ratio observed in the AB_2, Vf, and BB samples.

3) In the case of the STAR sample, the amount of Cu^{II} is definitely higher, being >60% on average. In STAR, the blue chromophore is Cu^{II} in a distorted (4 + 2) coordination in the glass, as indicated by EPR. The different results obtained in EXAFS analysis can simply be explained by the interference of both Cu^{I} and Cu^{II} structures signals, which are present in similar distances, and by

the fact that likely the two further oxygen atoms in the 4 + 2 coordination give rise to effects barely detectable.

Apparently, the deeper insight provided by the speciation information obtained through the XAS and EPR investigation allows one to go beyond the sample classification achievable using only a chemical basis [51]. Accordingly, the data presented here suggest that the samples which could be classified as either Co-Cu (AB_2, Vf, BB) or Cu (AB_9, STAR) blue colored materials, are effectively representing a more complex variety of situations.

With this respect, under the authors' opinion appears worthy of noting that the 5 samples here studied depict a variegated situation also concerning the technological processes used to create the products. In particular, without reference to the additional presence of Co, 4 out of the 5 samples present almost similar Cu^{II}/Cu^{I} ratio values. This information could suggest a similar condition of glass manufacturing. According to e.g. Hunault et al. [52], in fact, Co^{II} can be found associated with Cu^{I} in an almost wide variety of oxygen fugacities and/or temperature values. According to this consideration, the colour hue in these four samples could be obtained by properly adding either Co or Cu sources in the appropriate amount.

Conversely, to achieve a favourable Cu^{II} excess ratio, as found in the STAR sample, a different set of temperatures and/or oxygen fugacities would have been required. It is also worth noting that the heterogeneity in the blue hue of the STAR sample (Fig. S8) appears to have been intentionally introduced by the manufacturer to improve its aesthetic quality. The lighter portion reveals a lower total Copper content (Table 1), but also a reduced amount of Cu^{II}, revealed by the XANES point analyses (Table 3). Conversely, the Co content is held constant (at the level of an impurity) in the whole sample.

According to these experimental evidences, a change of the redox speciation in the molten glass could have been realized through the addition of a reducing agent, as e.g. plant ashes, followed by rapid quenching of the inhomogeneous melt.

5. Conclusions

This spectroscopic approach, combining XAS and EPR techniques, resulted successful in the characterization of the origin of the Co- and Cu-based blue colors in the Bronze Age Paduli glasses, highlighting the high skill reached in their production. The XAS spectra provided significant information on one hand, confirming the presence of the Co^{II} chromophore, in the samples where this species is chemically more abundant. On the other hand, the presence of the Cu^{II} chromophore was identified and quantified, while monitoring the variable occurrence of these species allowed monitoring the sample inhomogeneity. Cu^{II}, as revealed by EPR, appears in a distorted (4 +2)-fold coordination and it is suggested that it could also partly occur clustered to form pairs. This findings confirm the complementarity of XAS and EPR analyses.

The blue hue of the investigated samples is, in general, naturally due to the presence of either Co^{II} and/or Cu^{II} in their respective 4-fold and 4+2-fold coordinated environment in the glass, without requiring an intentional control of the firing conditions. Conversely, at least in the case of the STAR sample, we can presume that the redox buffer has been shifted towards more oxidising conditions, which were then modulated by the addition of reducing materials to induce aesthetic effects in the glass.

CRediT authorship contribution statement

Jacopo Orsilli: Writing – original draft, Visualization, Validation, Methodology, Investigation. **Silvia Vettori:** Writing – review & editing, Writing – original draft, Visualization, Validation, Supervision, Investigation, Conceptualization. **Francesca Giannetti:** Writing – review & editing, Writing – original draft, Validation, Investigation. **Emma Cantisani:** Writing – review & editing, Writing – original draft, Visualization, Validation, Investigation, Conceptualization. **Rachele Manganelli Del Fà:** Writing – review & editing, Writing – original draft, Visualization, Methodology. **Cesare Carlo Allart:** Investigation. **Francesco D'Acapito:** Writing – review & editing, Writing – original draft, Validation, Investigation. **Francesco Di Benedetto:** Writing – review & editing, Writing – original draft, Visualization, Validation, Supervision, Methodology, Investigation, Funding acquisition, Conceptualization.

Declaration of competing interest

The authors declare the following financial interests/personal relationships which may be considered as potential competing interests: Francesco Di Benedetto reports financial support was provided by University of Ferrara Department of Physics and Earth Sciences. If there are other authors, they declare that they have no known competing financial interests or personal relationships that could have appeared to influence the work reported in this paper.

Acknowledgements

ESRF is kindly acknowledged for provision of synchrotron radiation during the HG217 beamtime. Alessandro Puri is also thanked for its support during the beamtime. Prof. Sandra Ristori is gratefully acknowledged for granting access to the EPR laboratory at the Department of Chemistry of the University of Florence. Stefano Di Benedetto is ackowledged for realising the sample holder using his 3D printing facility. FDB acknowledges the FAR2023 and FAR2024 funds for the University of Ferrara.

Appendix A. Supplementary data

Supplementary data to this article can be found online at https://doi.org/10.1016/j.talanta.2026.129622.

Data availability statement

XAS data collected at BM08 in the experiment HG217 are deposited in the ESRF DATA Repository doi.esrf.fr/10.15151/ESRF-ES-1334151285. EPR data can be provided upon request to the authors.

References

[1] J. Henderson, Ancient Glass, Cambridge university press, Cambridge New York, 2013.

[2] I. Angelini, B. Gratuze, G. Artioli, Glass and other vitreous materials through history, in: Contrib. Mineral. Cult. Herit., Mineralogical Society of Great Britain and Ireland, 2019, pp. 87–150, https://doi.org/10.1180/EMU-notes.20.3.

[3] W. Turner, Studies of ancient glasses and glassmaking processes. Part IV. The chemical composition of ancient glasses, Journal of the Society of Glass Technology 40 (1956) 162T–186T.

[4] E.V. Sayre, Summary of the brookhaven program of analysis of ancient glass, in: Appl. Sci. Exam, Works Art, P. England, Boston, 1965, pp. 145–154. https://scholar.google.com/scholar_lookup?title=Summary%20of%20the%20Brookhaven%20Program%20of%20analysis%20of%20ancient%20glass&publication_year=1965&author=E.%20Sayre. (Accessed 26 August 2025).

[5] Bernard Gratuze, Les Premiers Verres Au Natron Retrouvés En Europe Occidentale: Composition Chimique Et chrono-typologie, Ann. 17eme Congr. Assoc, Int. Pour Hist. Verre, 2009, pp. 8–14.

[6] R.H. Doremus, Glass Science, second ed., John Wiley, New York, 1973.

[7] J. Henderson, The raw materials of early glass production, Oxf. J. Archaeol. 4 (1985) 267–291, https://doi.org/10.1111/j.1468-0092.1985.tb00248.x.

[8] I. Freestone, Looking into glass, free. 1991 look. Glass Sci. past Ed Bowman 37 57 Lond, Br. Mus. Press, 1991. https://www.academia.edu/4569306/Looking_into_Glass. (Accessed 26 August 2025).

[9] K. Nassau, The Physics and Chemistry of Color: the Fifteen Causes of Color, Wiley, New York, 2001.

[10] S. Quartieri, R. Arletti, G. Vezzalini, M. Dalconi, N. Giordani, Archaeometrical Analyses of Ancient Glass of the Imperial Age, 2004.

[11] F. D'Acapito, X-Ray absorption spectroscopy (XAS) applied to cultural heritage, in: Handb. Cult. Herit. Anal., Springer International Publishing, 2022, pp. 45–67.

[12] K. Janssens, M. Cotte, The Use of XAS and Related Methods in Cultural Heritage Investigations, 2023, pp. 1039–1046, https://doi.org/10.1107/S1574870720004802.
[13] S. Schöder, K. Müller, L. Tranchant, A. Rouquié, P. Gueriau, M. Thoury, E. Bérard, T. Okbinoglu, F. Berenguer, C. Iacconi, L. Robbiola, T. Moreno, S.X. Cohen, L. Bertrand, Heritage research at the PUMA beamline, Appl. Phys. A 130 (2024) 848, https://doi.org/10.1007/s00339-024-08026-0.
[14] J.P. Veiga, M.O. Figueiredo, Copper blue in an ancient glass bead: a XANES study, Appl. Phys. A 83 (2006) 547–550, https://doi.org/10.1007/s00339-006-3540-1.
[15] A. Santagostino Barbone, E. Gliozzo, F. D'Acapito, I. Memmi Turbanti, M. Turchiano, G. Volpe, The *sectilia* panels of faragola (ascoli satriano, southern Italy): a multi-analytical study of the red, orange and yellow glass slabs*, Archaeometry 50 (2008) 451–473, https://doi.org/10.1111/j.1475-4754.2007.00341.x.
[16] W. Klysubun, Y. Thongkam, S. Pongkrapan, K. Won-in, J. T-Thienprasert, P. Dararutana, XAS study on copper red in ancient glass beads from Thailand, Anal. Bioanal. Chem. 399 (2011) 3033–3040, https://doi.org/10.1007/s00216-010-4219-1.
[17] A. Silvestri, S. Tonietto, F. D'Acapito, G. Molin, The role of copper on colour of palaeo-christian glass mosaic tesserae: an XAS study, J. Cult. Herit. 13 (2012) 137–144, https://doi.org/10.1016/j.culher.2011.08.002.
[18] R. Arletti, S. Quartieri, I.C. Freestone, A XANES study of chromophores in archaeological glass, Appl. Phys. A 111 (2013) 99–108, https://doi.org/10.1007/s00339-012-7341-4.
[19] D.C. Koningsberger, R. Prins, X-ray Absorption: Principles, Applications, Techniques of EXAFS, SEXAFS and XANES, 1986. https://www.osti.gov/biblio/5927479. (Accessed 26 August 2025).
[20] A.K. Shukla, Spectroscopic Techniques for Archaeological and Cultural, IOP Publishing Ltd, Heritage Research, 2020, https://doi.org/10.1088/978-0-7503-2616-2.
[21] K. Polikreti, Y. Maniatis, A new methodology for the provenance of marble based on EPR spectroscopy, Archaeometry 44 (2002) 1–21, https://doi.org/10.1111/1475-4754.00040.
[22] L. Le Pape, Application of EPR in studies of archaeological samples, in: G.A. Webb (Ed.), Mod. Magn. Reson., Springer International Publishing, Cham, 2016, pp. 1–25, https://doi.org/10.1007/978-3-319-28275-6_30-1.
[23] C.B. Azzoni, D. Di Martino, C. Chiavari, M. Martini, E. Sibilia, M. Vandini, Electron paramagnetic resonance of mosaic glasses from the mediterranean area, Archaeometry 44 (2002) 543–554, https://doi.org/10.1111/1475-4754.00085.
[24] A.M. Jaia, C. Virili, A. Curci, F. Fiori, G. Di Pasquale, A. D'Auria, Il sito perilacustre di epoca protostorica di loc. Paduli (Colli sul Velino, RI). Indagini Di Superficie 2011-2013 E Saggio Di Scavo 2015, Preistoria E Protostoria in Etruria, 2020, pp. 415–444.
[25] Carlo Virili, La Piana di Rieti ed il bacino di Piediluco tra Bronzo Antico e Bronzo Medio: un lungo processo verso le prime forme di popolamento stabile e capillare del territorio, in: Lungo Il Corso Velino, Officina Edizioni, Roma, 2021, pp. 179–226.
[26] Carlo Virili, Paesaggi d'acqua velini: il sito perilacustre di località Paduli, in: Rieti Città Delle Acque Studi E Ric. Geol. Archeol, E Storia Dell'agro Reatino, Teseo Editore, Rieti, 2022, pp. 121–154.
[27] Carlo Virili, Alessandro M. Jaia, Alessandro Zanini, Emma Cantisani, Silvia Vettori, Lucia Vanacore, Alessia D'Auria, Il sito perilacustre di epoca protostorica di loc. Paduli (Colli sul Velino, RI). Indagini radiometriche, archeometriche e paleobotaniche. Atti PPE XIV, 2022, pp. 779–813.
[28] S. Vettori, F. Giannetti, E. Braschi, Riccardo Avanzinelli, Carlo Virli, Alessandro M. Jaia, Alessandro Zanini, Emma Cantisani, Bronze Age vitreous materials from Central Italy: a first insight through an interdisciplinary and multi analytical approach, J. Archaeol. Sci. Reports 67 (2025) 105396–105410.
[29] F. d'Acapito, G.O. Lepore, A. Puri, A. Laloni, F. La Manna, E. Dettona, A. De Luisa, A. Martin, The LISA beamline at ESRF, J. Synchrotron Radiat. 26 (2019) 551–558, https://doi.org/10.1107/S160057751801843X.
[30] B. Ravel, M. Newville, *Athena* , *Artemis* , *Hephaestus* : data analysis for X-ray absorption spectroscopy using *IFEFFIT*, J. Synchrotron Radiat. 12 (2005) 537–541, https://doi.org/10.1107/S0909049505012719.
[31] M. Newville, Larch: an analysis package for XAFS and related spectroscopies, J. Phys. Conf. Ser. 430 (2013) 012007, https://doi.org/10.1088/1742-6596/430/1/012007.
[32] A.L. Ankudinov, B. Ravel, J.J. Rehr, S.D. Conradson, Real-space multiple-scattering calculation and interpretation of x-ray-absorption near-edge structure, Phys. Rev. B 58 (1998) 7565–7576, https://doi.org/10.1103/PhysRevB.58.7565.
[33] I.S. Kotousova, S.M. Polyakov, Electron-diffraction study of Co3O4, Kristallografiya 17 (1972) 661–663.
[34] R.W.G. Wyckoff, Crystal Structures: 1, second ed., Interscience Publishers, New York, 1963, pp. 85–237.
[35] Von M.C. Neuburger, Praezisionsmessung der Gitterkonstante von Cuprooxyd Cu2O, Zeitschrift fur Physik (1930) 845–850.
[36] H.T. Evans, The Crystal Structures of Low Chalcocite and Djurieite, (n.d.).
[37] I.D. Brown, 14 - the bond-valence method: an empirical approach to chemical structure and bonding, in: M. O'Keeffe, A. Navrotsky (Eds.), Ind. Chem. Libr., Elsevier, 1981, pp. 1–30, https://doi.org/10.1016/B978-0-12-525102-0.50007-4.
[38] M. Newville, Using bond valence sums as restraints in XAFS analysis, Phys. Scr. (2005) 159, https://doi.org/10.1238/Physica.Topical.115a00159.
[39] M. Hunault, V. Vercamer, M.W. Haverkort, M.-A. Arrio, C. Brouder, G. Calas, A. Juhin, Tracking the signature of low symmetry environments in the XAS *K* pre-edge, J. Phys. Conf. Ser. 712 (2016) 012005, https://doi.org/10.1088/1742-6596/712/1/012005.
[40] G. Calas, L. Galoisy, L. Cormier, The color of glass, in: P. Richet, R. Conradt, A. Takada, J. Dyon (Eds.), Encycl. Glass Sci. Technol. Hist. Cult., first ed., Wiley, 2021, pp. 677–691, https://doi.org/10.1002/9781118801017.ch6.2.
[41] I. Cianchetta, I. Colantoni, F. Talarico, F. d'Acapito, A. Trapananti, C. Maurizio, S. Fantacci, I. Davoli, Discoloration of the smalt pigment: experimental studies and ab initio calculations, J. Anal. At. Spectrom. 27 (2012) 1941, https://doi.org/10.1039/c2ja30132f.
[42] E. Gliozzo, A. Santagostino Barbone, F. D'Acapito, M. Turchiano, I. Turbanti Memmi, G. Volpe, The *sectilia* panels of faragola (ascoli satriano, southern Italy): a multi-analytical study of the green, marbled (green and yellow), blue and blackish glass slabs, Archaeometry 52 (2010) 389–415, https://doi.org/10.1111/j.1475-4754.2009.00493.x.
[43] J. Finzel, K.M. Sanroman Gutierrez, A.S. Hoffman, J. Resasco, P. Christopher, S. R. Bare, Limits of detection for EXAFS characterization of heterogeneous single-atom catalysts, ACS Catal. 13 (2023) 6462–6473, https://doi.org/10.1021/acscatal.3c01116.
[44] J. Peisach, W.E. Blumberg, Structural implications derived from the analysis of electron paramagnetic resonance spectra of natural and artificial copper proteins, Arch. Biochem. Biophys. 165 (1974) 691–708, https://doi.org/10.1016/0003-9861(74)90298-7.
[45] S.K. Hoffmann, J. Goslar, S. Lijewski, A. Zalewska, EPR and ESE of CuS4 complex in Cu(dmit)2: g-Factor and hyperfine splitting correlation in tetrahedral Cu–sulfur complexes, J. Magn. Reson. 236 (2013) 7–14, https://doi.org/10.1016/j.jmr.2013.08.009.
[46] F. Bou-Abdallah, N.D. Chasteen, Spin concentration measurements of high-spin ($g' = 4.3$) rhombic iron(III) ions in biological samples: theory and application, JBIC, J. Biol. Inorg. Chem. 13 (2007) 15–24, https://doi.org/10.1007/s00775-007-0304-0.
[47] J. Svorec, M. Valko, J. Moncol, M. Mazúr, M. Melník, J. Telser, Determination of intermolecular copper–copper distances from the EPR half-field transitions and their comparison with distances from X-ray structures: applications to copper(II) complexes with biologically important ligands, Transit. Met. Chem. 34 (2009) 129–134, https://doi.org/10.1007/s11243-008-9168-6.
[48] F. Bardelli, G. Giuli, F. Di Benedetto, P. Costagliola, G. Montegrossi, V. Rimondi, M. Romanelli, L.A. Pardi, G. Barone, P. Mazzoleni, Spectroscopic study of volcanic ashes, J. Hazard. Mater. 400 (2020) 123213, https://doi.org/10.1016/j.jhazmat.2020.123213.
[49] M. Hunault, G. Calas, L. Galoisy, G. Lelong, M. Newville, Local ordering around tetrahedral Co^{2+} in silicate glasses, J. Am. Ceram. Soc. 97 (2014) 60–62, https://doi.org/10.1111/jace.12709.
[50] S. Quartieri, R. Arletti, The use of X–Ray absorption spectroscopy in historical glass research, in: K. Janssens (Ed.), Mod. Methods Anal. Archaeol. Hist. Glass, first ed., Wiley, 2013, pp. 301–309, https://doi.org/10.1002/9781118314234.ch13.
[51] M. Smirniou, Th Rehren, Shades of blue – cobalt-copper coloured blue glass from New Kingdom Egypt and the Mycenaean world: a matter of production or colourant source? J. Archaeol. Sci. 40 (2013) 4731–4743, https://doi.org/10.1016/j.jas.2013.06.029.
[52] M.O.J.Y. Hunault, C. Loisel, F. Bauchau, Q. Lemasson, C. Pacheco, L. Pichon, B. Moignard, K. Boulanger, M. Hérold, G. Calas, I. Pallot-Frossard, Nondestructive Redox quantification reveals glassmaking of rare French gothic stained glasses, Anal. Chem. 89 (2017) 6277–6284, https://doi.org/10.1021/acs.analchem.7b01452.